



Investigating effect of climate change on drought propagation from meteorological to hydrological drought using multi-model ensemble projections

Muhammad Jehanzaib¹ · Muhammad Nouman Sattar^{1,4} · Joo-Heon Lee² · Tae-Woong Kim³

Published online: 16 December 2019

© Springer-Verlag GmbH Germany, part of Springer Nature 2019

Abstract

Climate change is a main driving force that affects the hydrological cycle, leading to an increase in natural hazards. Among these natural hazards, drought is one of the most destructive and becomes more complex considering climate change. Therefore, it is necessary to investigate the effect of climate change on different types of drought. In this study, we examined the propagation probability of meteorological drought into hydrological drought using a probabilistic graphical model across South Korea. We performed correlation analyses among meteorological drought represented by Standardized Precipitation Index (SPI) and Standardized Precipitation Evapotranspiration Index (SPEI) and hydrological drought by Standardized Runoff Index (SRI) on different time scales. Drought characteristics were examined under a baseline period, RCP 4.5, and 8.5 climate change scenarios, and the results illustrated that drought characteristics varied spatially. On average, drought severity of SPI increased in P1 (2011–2040) and then decreased in P2 (2041–2070) and P3 (2071–2099) under RCP 4.5, whereas drought severity also increased in P1 under RCP 8.5. However, average drought severity of SPEI increased in P3, whereas that of SRI showed a decreasing trend for all the periods. Finally, propagation occurrence probabilities of different states of meteorological drought resulting in different states of hydrological drought were examined under climate change scenarios. The average propagation probability of extreme state of meteorological drought resulting in moderate and severe condition of hydrological drought increased by 13% and 2%, respectively, under RCP 4.5; while average propagation probability of extreme state of meteorological drought resulting in severe and extreme conditions of hydrological drought increased by 1.5% and 84%, respectively, under RCP 8.5. We concluded that propagation probability of meteorological drought into hydrological drought increased significantly under climate change. These findings will be helpful for early mitigation of hydrological drought.

Keywords Climate change · Drought propagation · Meteorological drought · Hydrological drought

1 Introduction

The consequences of climate change on the hydrological cycle and water resources lead to increase in extreme natural disasters, such as floods and droughts. Drought is a

Electronic supplementary material The online version of this article (<https://doi.org/10.1007/s00477-019-01760-5>) contains supplementary material, which is available to authorized users.

✉ Tae-Woong Kim
twkim72@hanyang.ac.kr

Muhammad Jehanzaib
jehanzaib7@hanyang.ac.kr

Muhammad Nouman Sattar
enr_nouman847@yahoo.com

Joo-Heon Lee
leejh@joongbu.ac.kr

¹ Department of Civil and Environmental Engineering, Hanyang University, Seoul 04763, Republic of Korea

² Department of Civil Engineering, Joongbu University, Goyang 10279, Republic of Korea

³ Department of Civil and Environmental Engineering, Hanyang University, Ansan 15588, Republic of Korea

⁴ School of Civil Engineering, The University of Faisalabad, Faisalabad 38000, Pakistan

complex natural process that primarily occurs due to less than normal precipitation for several months or years (Dai 2012). Although drought is mainly caused by lack of precipitation, other factors, such as temperature and wind speed, are certainly involved in drought occurrence (Rhee and Cho 2016). The increase in temperature enhances evapotranspiration, which results in increased drought risk for the twenty-first century around the world. Drought is divided into four types: meteorological, agricultural, hydrological and socio-economic drought (Wilhite and Glantz 1985). In general, the latter three types of drought are directly or indirectly linked to meteorological drought through variables such as precipitation, soil moisture, overland flow, infiltration, groundwater discharge, evaporation and streamflow, which are all involved in the hydrological cycle (Zhao et al. 2014). Detailed insight is required to understand the associated linkages between different types of drought to cope with drought-induced disasters (Mishra et al. 2010).

Over the recent decades, various drought monitoring indices including the Standardized Precipitation Index (SPI), Rainfall Anomaly Index (RAI), Reconnaissance Drought Index (RDI), Z-index, Standardized Precipitation Evapotranspiration Index (SPEI), Palmer Drought Severity Index (PDSI), and Standardized Runoff Index (SRI) have been developed to assess meteorological and hydrological droughts (Palmer 1965; Van-Rooy 1965; Zhensheng and Yuguo 1990; McKee et al. 1993; Tsakiris and Vangelis 2005; Shukla and Wood 2008; Vicente-Serrano et al. 2010). Among the above-mentioned indices, standardized drought indices have been extensively used due to their flexibility and simplicity in computing drought on different time scales with limited data requirements and comparability in time and space (Zhao et al. 2014).

Numerous studies have focused on an individual type of drought, whereas few studies have investigated the relationship between meteorological and hydrological droughts because of the complex mechanism of drought propagation (Mishra et al. 2010; Wang et al. 2016a). Zhao et al. (2014) investigated the effects of meteorological drought on hydrological droughts in the Jinghe River Basin, China, and concluded that frequency of hydrological drought was less than that of meteorological drought, but magnitude and duration of hydrological drought were greater than those of meteorological drought. Van Loon and Van Lanen (2012) investigated drought propagation using meteorological and hydrological variables and computed basic features of drought propagation, such as lag time, pooling, and lengthening. Huang et al. (2017) used the SPI and SSI indices to estimate meteorological and hydrological droughts in the Wei River Basin, China, and concluded that propagation time of meteorological and hydrological droughts follows a seasonal trend. Spring and summer

seasons resulted in a short propagation time, and a long propagation time is observed in winter and autumn.

Melo and Wendland (2016) found lag times between meteorological and hydrological droughts using change point analysis. Shin et al. (2018a) assessed meteorological and hydrological droughts using the SPI and Palmer Hydrological Drought Index (PHDI), calculated the propagation probability using the conditional probability theory, and found that 33% of meteorological drought on a 3-month time scale and 48% on a 6-month time scale were propagated into hydrological drought. Sattar and Kim (2018) determined the lag time between meteorological and hydrological droughts at different intensities of meteorological drought using the Bayesian network model. Rhee and Cho (2016) investigated future changes of drought characteristics in South Korea using a multi-model ensemble (MME) projection and concluded that drought frequency is projected to increase in the future, while drought frequency was observed to decrease. The General Circulation Model (GCM) and Regional Circulation Model (RCM) produce climate data, which are used to calculate drought indices under different climate change scenarios. Orłowsky and Seneviratne (2013) analyzed future trends of meteorological and agricultural droughts using the fifth phase of the Coupled Model Intercomparison Project (CMIP5) projections and concluded that there was no increase in drought occurrence in East Asia.

In the context of future global warming due to increase in greenhouse gases (IPCC 2013), there is need to assess how climate change is affecting different types of drought, their characteristics, and linkages between drought types. Ghosh and Mujumdar (2007) noted that the results of GCM simulation may lead to high uncertainty due to an uncertain future scenario and incomplete knowledge about the geophysical processes of global change. It is very difficult to assess changes in drought characteristics under climate change on the Korean peninsula due to large variability on both the temporal and regional scales. The sensitivity of South Korea to global warming has been found to be very model dependent in multiple analyses, which means that different models gave different results in response to increased greenhouse gas emissions (Lee et al. 2019). Use of MME usually improves the efficiency of forecast and consistency of individual models (Ouyang et al. 2015; Wang et al. 2016b; Yu et al. 2017).

The aim of this study is to elucidate the effects of climate change using an MME projection on propagation of meteorological drought into hydrological drought under different climate change scenarios. There have been several studies that discuss drought propagation. However, there have only been a few studies that discuss the effects of changing climate on drought characteristics using MME projections (Rhee and Cho 2016; Lee et al. 2019). The

novel feature of this study is the use of the probabilistic graphical model (PGM) to determine the propagation probability of classes of meteorological drought into hydrological drought using MME projections under different climate change scenarios. The main objectives of this study are: (1) to analyze spatial variation in drought characteristics of different drought types using MME projections under climate change scenarios (RCP 4.5 and 8.5) and (2) to estimate propagation probability of different classes of meteorological drought into hydrological drought according to different climate change scenarios.

2 Materials and methods

2.1 Study area

The Korean Peninsula is located between 37° north latitude and 127° 30' east longitude. According to climate conditions, South Korea exhibits four distinct seasons with long summer and winter seasons and brief fall and spring seasons. The average annual precipitation ranges between 1200 and 1400 mm, of which 50–60% falls in the summer (June, July, and August). Average annual temperature varies between 10 and 14 °C.

This study was conducted in the five main river basins of South Korea as presented in Fig. 1. The land area of the basins ranged between 3469 and 34,428 km². The study areas were totally covered with 1.61% bare land, 2.1% grassland, 2.6% water bodies, 5.5% urbanized area, 24% agricultural fields, and 62% forest on average.

2.2 Data

In this study, monthly meteorological data of precipitation and temperature were collected for the period of 1981–2010 from 56 weather stations, managed by the Korea Meteorological Administration. Meteorological data were areal-averaged by Thiessen's polygon method and converted into basin scale. Monthly streamflow data of five basins for the period of 1981–2010 were collected from the Water Resources Management Information System (WAMIS) (<http://www.wamis.go.kr>).

To assess the influence of climate change, daily precipitation data of five general circulation models (GCMs) were downloaded from the Earth System Grid Federation website (<https://esgf-node.llnl.gov>) for the period of 2011–2099 under Representative Concentration Pathway (RCP) 4.5 and 8.5, and used for calculating meteorological drought indices. The downloaded data were bias-corrected and downscaled by combining quantile delta mapping (QDM) and bias corrected spatial downscaling (BCSD).

More details about downscaling and bias correction procedure can be found in Eum and Cannon (2017).

The daily streamflow data for the period of 2011–2099 were obtained from the WAMIS, which were simulated by the precipitation runoff modeling system (PRMS). The PRMS generates streamflow after considering the effect of dams and reservoirs. The daily streamflow data used in this study were simulated by the PRMS using daily precipitation data of five GCMs as input, and used for computing a hydrological drought index.

Climate change is projected to cause an escalation in climatic variation coupled with increasing uncertainty. The uncertainties in emission scenarios are more limited than those from the climate models (Xu et al. 2018). MME projections have the potential to combine the strengths of individual models and to better represent forecast uncertainty than the use of a single model (Shin et al. 2018b). The ensemble of five GCMs was computed such that each model was assumed to be independent and given equal weight. These MME projections were further used to investigate the individual impacts of RCP 4.5 and 8.5 scenarios on drought characteristics and propagation. The details of the five GCMs are shown in Table 1.

2.3 Meteorological drought indices

2.3.1 Standardized Precipitation Index (SPI)

The SPI is a very popular drought index used to identify meteorological drought. Computation of SPI is simple because it only depends on precipitation. In this study, daily precipitation data were aggregated into monthly time scales, and fitted to a two-parameter gamma distribution function, as given in Eq. (1).

$$f(x; \alpha, \beta) = \frac{1}{\beta^\alpha \int_0^\infty x^{\alpha-1} e^{-x/\beta} dx} x^{\alpha-1} e^{-x/\beta}, \quad \text{for } x > 0 \quad (1)$$

where x is monthly precipitation, and α and β are shape and scale parameters of probability distribution, respectively. The parameters were estimated by the most widely used maximum likelihood estimation (MLE) method. The gamma probabilities were then transformed into a standard normal variate having a mean value of zero and a standard deviation of one (Vicente-Serrano et al. 2010).

2.3.2 Standardized Precipitation Evapotranspiration Index (SPEI)

Vicente-Serrano et al. (2010) suggested a drought index for monitoring meteorological drought based on a similar concept to that of SPI but that also considers potential evapotranspiration. The SPEI can be used to assess dry and wet periods on different timescales similar to the SPI.

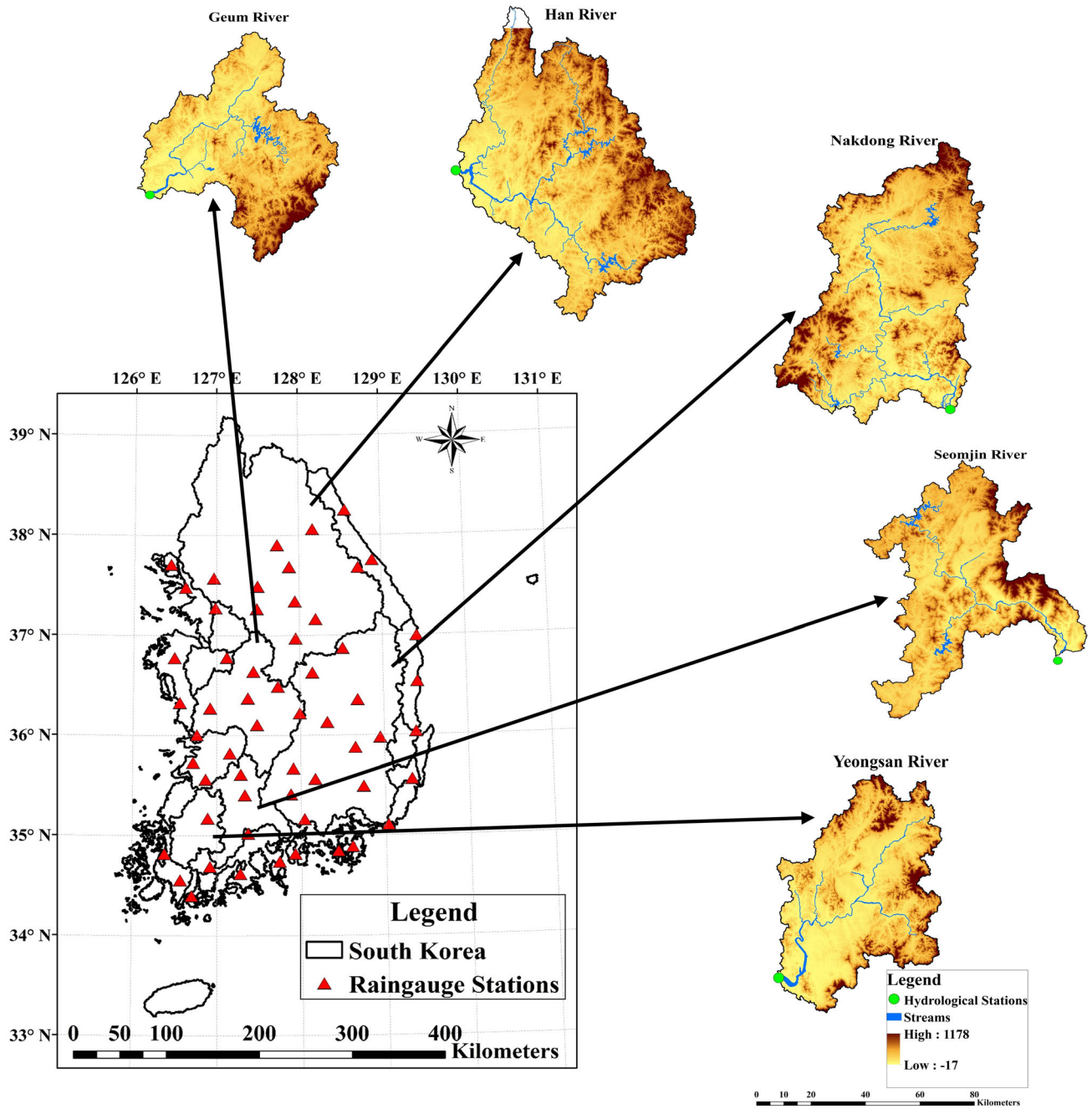


Fig. 1 Locations of study areas with weather stations, stream network, and topography

Table 1 Descriptions of the five global circulation models (GCMs) used in this study

GCMs	Institutes	Resolution
GFDL-ESM2M	NOAA Geophysical Fluid Dynamics Laboratory	2.5° × 2.023°
HadGEM2-ES	Met Office Hadley Centre	1.875° × 1.250°
IPSL-CM5A-LR	Institute Pierre-Simon Laplace	3.750° × 1.895°
MIROC-ESM-CHEM	JAMSTEC, NIES, AORI	2.813° × 2.791°
NorESM1-M	Norwegian Climate Centre	2.5° × 1.895°

Using monthly precipitation (P_i) and potential evapotranspiration (PET_i), the water balance (WB_i) is calculated through simple subtraction, as shown in Eq. (2).

$$WB_i = P_i - PET_i \tag{2}$$

The ensemble of PET was calculated by two methods. The Thornthwaite equation requires temperature and latitude as input and the Hargraves equation requires maximum and minimum temperature and latitude as input. The water balance WB_i was fitted to a three parametric log-logistic distribution as described by Vicente-Serrano et al. (2010), as given in Eq. (3).

$$f(x; \alpha, \beta, \gamma) = \frac{\left(1 + \frac{\gamma(x-\alpha)}{\beta}\right)^{-(1/\gamma+1)}}{\beta \left[1 + \left(1 + \frac{\gamma(x-\alpha)}{\beta}\right)^{-1/\gamma}\right]^2}, \tag{3}$$

where x is the water balance (WB), and α , β and γ are location, scale and shape parameters respectively. The parameters of probability distribution were calculated by the MLE method. The log-logistic probabilities were then transformed into standard normal distribution.

2.4 Hydrological Drought Index

The SRI was proposed by Shukla and Wood (2008) to characterize hydrological drought. Computation of SRI is quite similar to that of SPI, but it considers streamflow data instead of precipitation. Streamflow data were fitted to log-normal distribution, as given in Eq. (4).

$$f(x; \mu, \sigma) = \frac{1}{x} \cdot \frac{1}{\sigma\sqrt{2\pi}} \exp\left(-\frac{(\ln x - \mu)^2}{2\sigma^2}\right), \text{ for } x > 0 \tag{4}$$

where x is streamflow, and μ and σ are location and scale parameters estimated by the MLE method. The probabilities were transformed into standard normal distribution. The states of standardized drought indices based on severity are shown in Table 2.

2.5 Probabilistic graphical model

The PGM expresses a conditional dependence structure between random variables in the form of a graph. Bayesian networks lie in the category of PGM that encodes

Table 2 Classification of states of drought indices according to severity

SPI/SPEI/SRI	States
≤ -0.99	Normal
-1.49 to -1	Moderate
-1.99 to -1.5	Severe
≥ -2.0	Extreme

conditional probability between a set of learning variables in a direct acyclic graph (DAG), which is made up of two component nodes and links among them, as shown in Fig. 2. In this study, each node represented a variable, such as SPI or SPEI and SRI according to our study, and links were added between these nodes to indicate that one was directly influencing the other, although the states of each drought type differed among these nodes. This means that each individual class of hydrological drought depends on each individual class of meteorological drought. The parameters of Bayesian networks were estimated by the MLE, and the Hill-Climbing algorithm was used to learn the network using an R package. The general expression for conditional probabilities is given in Eq. (5).

$$P(H_i \in C_m | M_j \in C_m) = \frac{P(H_{i,m}, M_{j,m})}{P(M_j)} \tag{5}$$

where $P(HIM)$ is the propagation probability, C_m is drought class ($C_1 =$ no drought, $C_2 =$ moderate drought, $C_3 =$ severe drought, $C_4 =$ extreme drought), $P(M, H)$ is the joint probability, and $P(M)$ is the probability of meteorological drought. The probability of each class of hydrological drought given by each class of meteorological drought was calculated using the Bayesian network model.

3 Results and discussion

To understand the phenomenon of drought propagation, meteorological and hydrological drought indices were calculated on various time scales (1–12 months) using the SCI (Standardized Climate Indices) package in R (Stagge et al. 2015), and a threshold of -0.8 was selected to indicate drought as suggested by Yuan et al. (2016), Hao et al. (2017), and Wu et al. (2018). To identify the relationship between meteorological and hydrological droughts, the meteorological drought indices on 4-month time scale was selected as the most appropriate meteorological drought that had the highest Pearson correlation coefficient with the SRI on one-month time scale.

3.1 Spatial pattern of changes in mean drought characteristics under climate change

The results of MME projection showed a warmer climate over the South Korea with a temperature increase of $2.8\text{--}3.4\text{ }^\circ\text{C}$ and $5.2\text{--}5.8\text{ }^\circ\text{C}$ under RCP 4.5 and RCP 8.5 scenarios, respectively. To examine the effects of climate change on drought characteristics, data were divided into four periods: P0 (1981–2010) was selected as the baseline period, and the results of the other three periods: P1, P2, and P3 (2011–2040, 2041–2070 and 2071–2099,

Fig. 2 Schematic diagram of a probabilistic graphical model

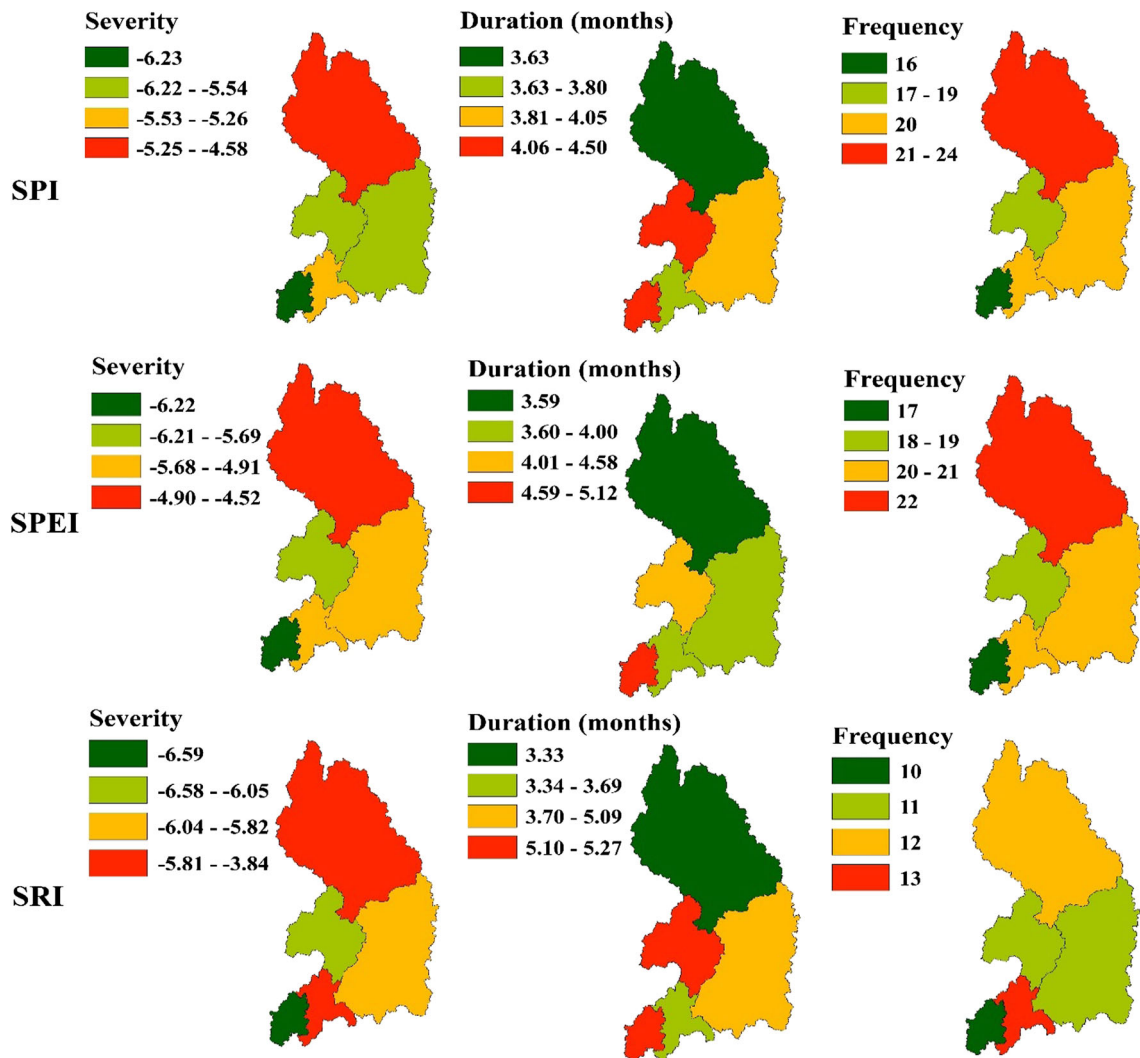
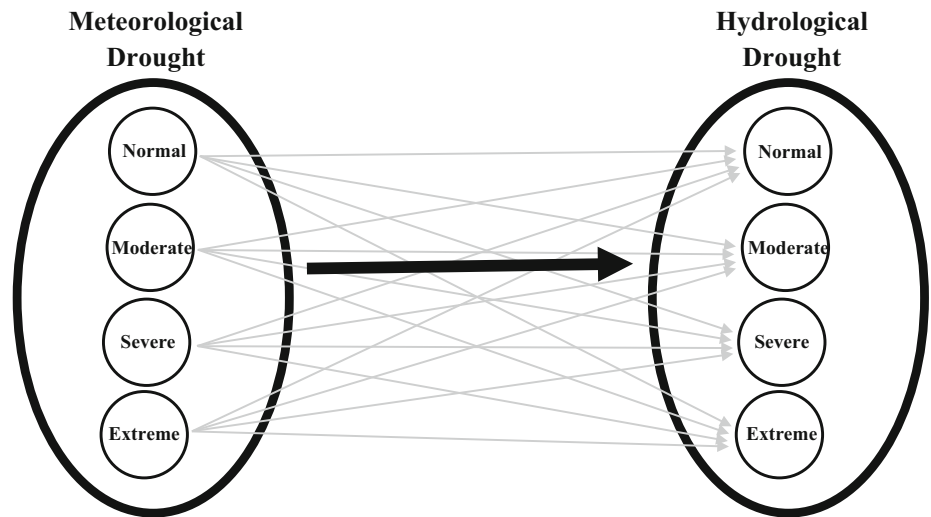


Fig. 3 Spatial analysis of meteorological and hydrological drought characteristics during the baseline period (1981–2010)

respectively) were compared with that of the baseline period. Spatial variations in the drought characteristics of SPI, SPEI, and SRI in the baseline period are depicted in Fig. 3. Drought characteristics varied spatially due to the heterogeneous geographical features among catchments.

The comprehensive results of comparative analysis between the baseline period and future periods in the Han River Basin showed that, in the case of SPI, drought severity increased 32.8% in P1, decreased 16.4% in P2, and decreased 30% in P3 under the RCP 4.5 scenario, whereas drought severity increased 23.6% in P1, increased 1% in P2, and decreased 1.7% in P3 under the RCP 8.5 scenario. Similarly, the SPEI showed that drought severity in the Han River Basin increased 15.4% in P1, decreased 24.7% in P2, and decreased 11.5% in P3 under the RCP 4.5 scenario, but drought severity decreased 37.9% in P1, decreased 1.6% in P2, and increased 57.9% in P3 under RCP 8.5 scenario. In the case of SRI, drought severity in the Han River Basin increased 26% in P1, decreased 38.4% and 13.3% in P2 and P3, respectively, under the RCP 4.5 scenario, whereas drought severity decreased in P1 and P2 (1.3% and 46.3%) and increased in P3 (29.3%) under the RCP 8.5 scenario. These results are in agreement with Lee and Kim (2013). In the Nakdong River Basin, the results of SPI revealed that drought severity increased 20% in P1, decreased 33.4% in P2 and P3 under the RCP 4.5 scenario, respectively, whereas drought severity increased 6.97% in P1 and decreased 41.7% and 21.9% in P2 and P3 under the RCP 8.5 scenario. Similarly, the SPEI showed that drought severity increased 11.8% in P1 and decreased 17.6% and 2.6% in P2 and P3, respectively, under the RCP 4.5 scenario, but drought severity decreased – 0.08% in P1, decreased 25.90% in P2, and increased 45.11% in P3 under the RCP 8.5 scenario. In the Nakdong River Basin, the severity of SRI increased 24.6% in P1 and decreased 56.1% and 18.3% in P2 and P3, respectively under the RCP 4.5 scenario, whereas drought severity decreased 40.2%, 62.9%, and 17.9% in P1, P2, and P3, respectively, under the RCP 8.5 scenario. The Geum

River Basin showed a similar trend to that in the Nakdong River Basin with different percentage of increase and decrease in drought severity. These findings are in accordance with those of Rhee and Cho (2016). The percentages of increase and decrease in drought characteristics in the Yeongsan River Basin under the two RCP scenarios are presented in Tables 3 and 4. Drought characteristics in the Seomjin River Basin indicated a similar trend to those in the Yeongsan River Basin with different percentages of increase and decrease in drought severity.

3.2 Linkage between meteorological and hydrological droughts

We compared two meteorological drought indices, SPI (4-month) and SPEI (4-month) with a hydrological drought index [SRI (1-month)] to investigate the phenomenon of drought propagation. Figure 4 illustrates different states of SPI (4-month) and SPEI (4-month) propagated into SRI (1-month) in the baseline period. Comprehensive analysis showed that hydrological drought lagged behind meteorological drought by 95 days on average. The results of our study are in agreement with those of Zhao et al. (2014), which demonstrated that the SRI lagged behind the SPI by 127 days. This property of lagging between meteorological and hydrological droughts depends on catchment characteristics such as storage capacity, topography, soil, land use, and land cover.

To examine the influence of climate change on drought propagation, the SPI (4-month) and the SPEI (4-month) were compared with the SRI (1-month) under the RCP 4.5 and RCP 8.5 scenarios. The results of meteorological drought events that propagated into hydrological drought in the Yeongsan River Basin are presented in Fig. 5. The outcomes of drought propagation showed that, on average, the SRI (1-month) lagged behind the SPI (4-month) and the SPEI (4-month) by 45 and 50 days, respectively, under the RCP 4.5 scenario. Similarly, the SRI (1-month) lagged

Table 3 Comparison of drought characteristics in the Yeongsan River Basin between the baseline and future periods under the RCP 4.5 scenario

Indices	Period	Drought characteristics		
		Severity (%)	Duration (%)	No. of droughts (%)
SPI	2011–2040	– 5.35	– 4.00	56.25
	2041–2070	– 33.04	– 25.15	18.75
	2071–2099	– 55.13	– 46.91	12.50
SPEI	2011–2040	– 16.82	– 21.84	17.65
	2041–2070	– 19.63	– 24.92	11.76
	2071–2099	– 34.01	– 35.80	23.53
SRI	2011–2040	– 14.36	– 14.20	30.00
	2041–2070	– 48.47	– 38.46	0.00
	2071–2099	– 52.94	– 48.72	– 10.00

Table 4 Comparison of drought characteristics in the Yeongsan River Basin between the baseline and future periods under the RCP 8.5 scenario

Indices	Period	Drought characteristics		
		Severity (%)	Duration (%)	No. of droughts (%)
SPI	2011–2040	9.56	21.11	25.00
	2041–2070	– 37.70	– 21.57	6.25
	2071–2099	– 19.94	– 18.52	– 6.25
SPEI	2011–2040	– 41.82	– 43.82	– 5.88
	2041–2070	– 41.01	– 35.21	11.76
	2071–2099	– 9.21	– 18.22	58.82
SRI	2011–2040	– 29.41	– 14.34	10.00
	2041–2070	– 54.86	– 39.56	– 30.00
	2071–2099	– 29.92	– 34.29	20.00

behind the SPI (4-month) and the SPEI (4-month) by 42 and 51 days, on average respectively, under the RCP 8.5 scenario. Due to an increase in temperature, the lag time between meteorological and hydrological droughts decreases significantly under both climate change scenarios.

3.3 Drought propagation probability under climate change scenarios

We estimated the propagation probability of meteorological drought conditioned on hydrological drought occurrence using a PGM. Hydrological drought is a later

occurring phenomenon than meteorological drought as illustrated by Van Loon and Van Lanen (2012). In this study, we estimated the drought propagation probability of classes of meteorological drought into classes of hydrological drought. First, we examined the drought propagation probability of SPI and SPEI into SRI in the baseline period of 1981–2010. The conditional probability of all states of SPI given different conditions of SRI in all the basins is shown in Fig. 6a. The results showed that the average conditional probability of the normal state of SPI resulting in normal conditions of SRI was greater than 97%, whereas the probability of the moderate state of SPI given moderate conditions of SRI was 35%. In addition,

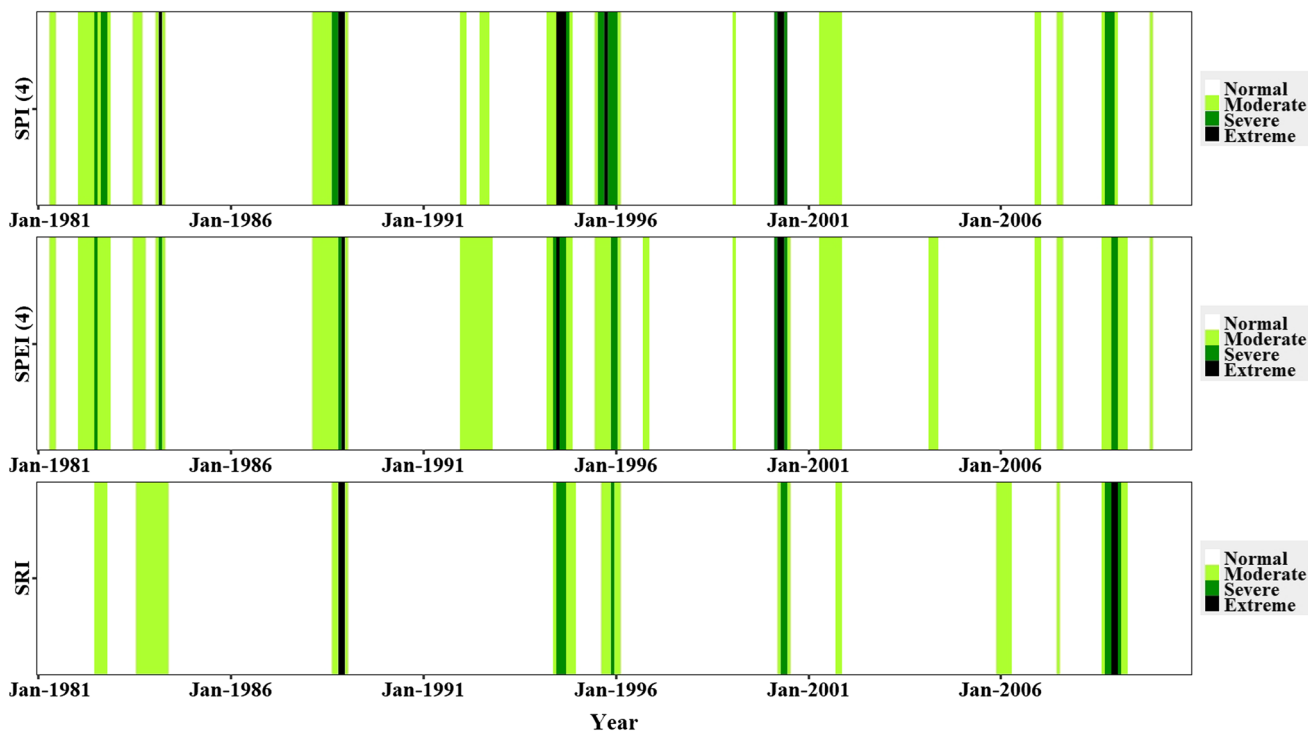


Fig. 4 States of drought in the baseline period in the Yeongsan River Basin

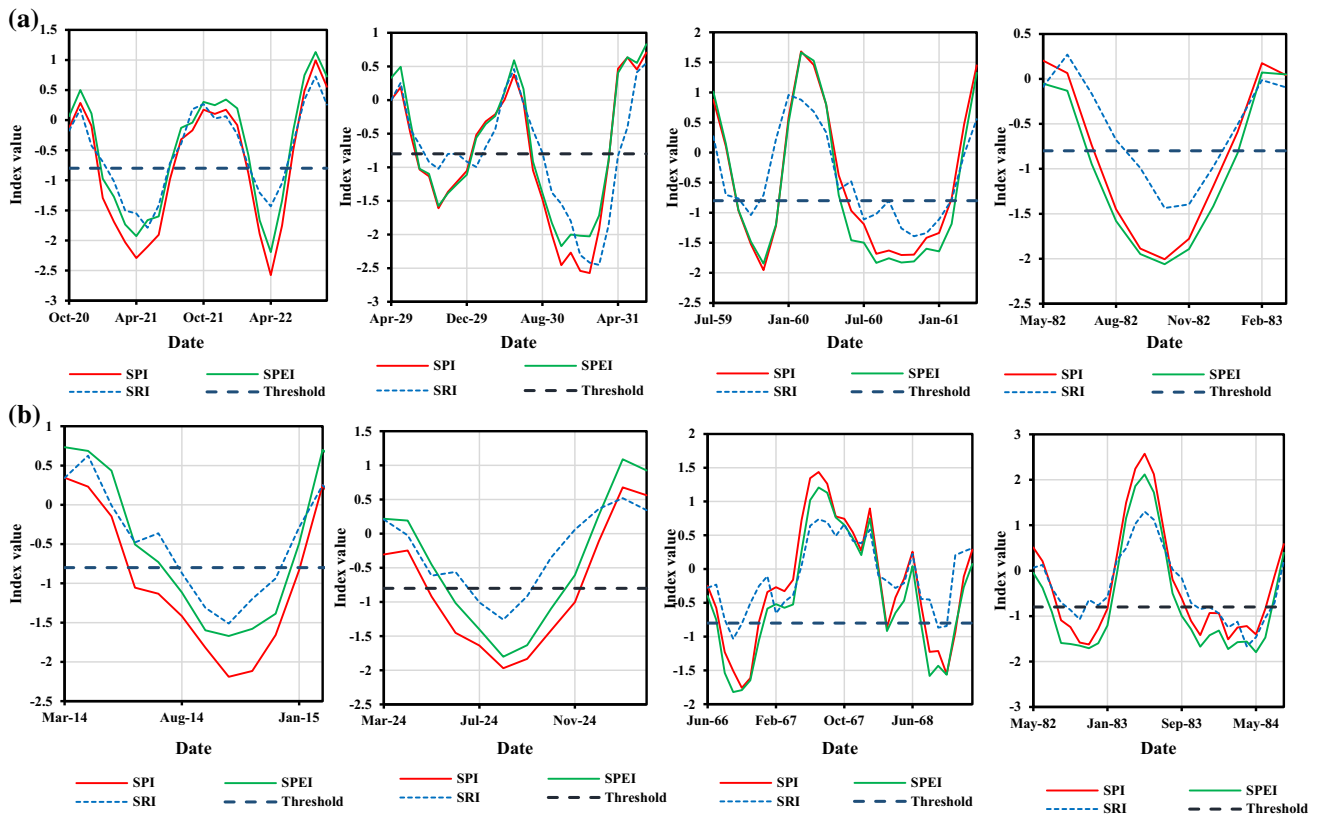


Fig. 5 Events that show hydrological drought in the Yeongsan River Basin lagging behind meteorological drought under the **a** RCP 4.5 and **b** RCP 8.5 scenarios

the probabilities of the severe and extreme states of SPI resulting in severe and extreme conditions of SRI were 14% and 16%, respectively. The average conditional probabilities of the severe state of SPI given moderate and extreme conditions of SRI were 49% and 2%, respectively, but the average conditional probabilities of the extreme state of SPI given moderate and severe conditions of SRI were 51% and 33%.

On the other hand, the average conditional probability of the normal state of SPEI given normal conditions of SRI was greater than 97%, whereas the probability of the moderate state of SPEI given moderate conditions of SRI was 37%. The average propagation probabilities of the severe and extreme states of SPEI given severe and extreme conditions of SRI were 27% and 12%, respectively. The average conditional probabilities of the severe state of SPEI given moderate and extreme conditions of SRI were 45% and 8%, respectively; however, the average conditional probabilities of the extreme state of SPEI given moderate and severe conditions of SRI were 25% and 57%, respectively. The propagation probabilities of all states of SPEI resulting different conditions of SRI in all the basins are shown in Fig. 6b.

Similarly, drought propagation probability was examined under two climate change scenarios. The results of conditional probability of SPI given SRI and that of SPEI given SRI under the RCP 4.5 scenario are illustrated in Tables 5 and 6, respectively. The average propagation probabilities of the severe and extreme states of SPI resulting in severe and extreme conditions of SRI were 14% and 7%, respectively. Meanwhile, the average conditional probabilities of the severe and extreme states of SPEI given severe and extreme conditions of SRI were 18% and 12%, respectively, under the RCP 4.5. In the case of RCP 8.5, the outcomes of propagation occurrence probability of SPI to SRI and SPEI resulting in SRI are shown in Tables 7 and 8, respectively. The average propagation occurrence probabilities of the severe and extreme states of SPI resulting in severe and extreme conditions of SRI were 10% and 25%, respectively, whereas the average propagation probabilities of the severe and extreme states of SPEI given severe and extreme conditions of SRI were 12% and 26%, respectively. The results of our study regarding propagation are in agreement with those of Shin et al. (2018a). The propagation probabilities of individual classes of SPI contributing toward SRI were observed under different climate change scenarios.

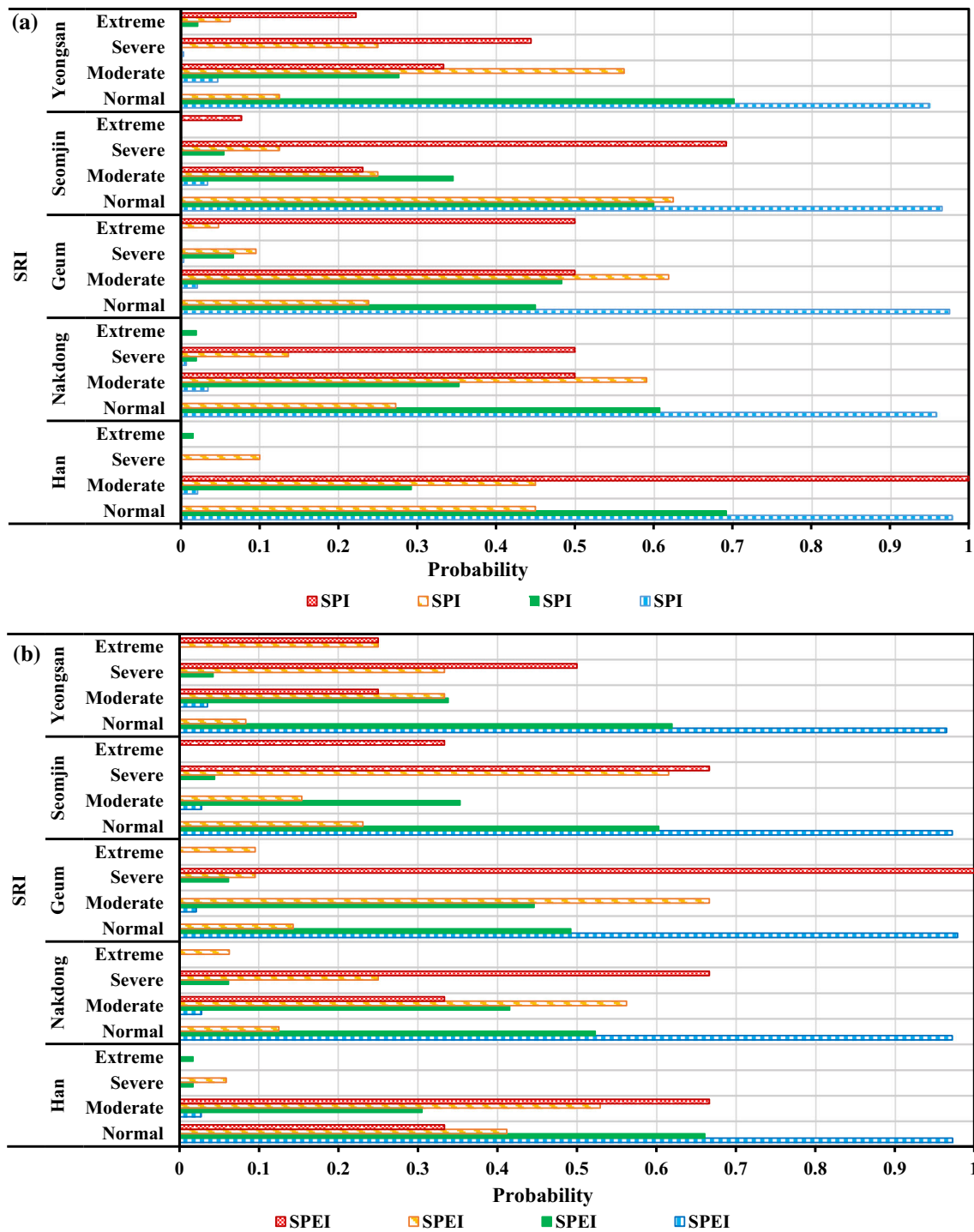


Fig. 6 Propagation probability of a SPI into SRI and b SPEI into SRI during the baseline period

3.4 Discussion

We examined the influence of climate change on drought characteristics using multiple drought indices and MME projections under the RCP 4.5 and RCP 8.5 scenarios. The novel feature of this study was to investigate probabilistic relationship between different states of meteorological and

hydrological droughts using the PGM. Climate is a crucial factor affecting drought characteristics. In this study, the drought characteristics represented by the SPI, SPEI and SRI varied spatially due to heterogeneous catchment characteristics such as geology of catchment, land use/cover, different soil types, and topography. Drought distorts the normal hydrological cycle due to a deficiency in

Table 5 Propagation probability of different classes of SPI into SRI under the RCP 4.5 scenario

Basin	SRI	SPI			
		Normal	Moderate	Severe	Extreme
Han River	Normal	0.99	0.73	0.14	0
	Moderate	0.01	0.26	0.66	0.62
	Severe	0	0.01	0.14	0.38
	Extreme	0	0	0.06	0
Nakdong River	Normal	0.99	0.63	0.16	0
	Moderate	0.01	0.35	0.68	0.40
	Severe	0	0.02	0.13	0.53
	Extreme	0	0	0.03	0.07
Geum River	Normal	0.98	0.76	0.07	0
	Moderate	0.02	0.21	0.69	0.31
	Severe	0	0.03	0.21	0.63
	Extreme	0	0	0.02	0.06
Seomjin River	Normal	0.99	0.73	0.07	0
	Moderate	0.01	0.26	0.76	0.47
	Severe	0	0.01	0.16	0.41
	Extreme	0	0.01	0.02	0.12
Yeongsan River	Normal	0.98	0.74	0.07	0
	Moderate	0.02	0.23	0.83	0.29
	Severe	0	0.03	0.07	0.59
	Extreme	0	0	0.02	0.12

Table 6 Propagation probability of different classes of SPEI into SRI under the RCP 4.5 scenario

Basin	SRI	SPEI			
		Normal	Moderate	Severe	Extreme
Han River	Normal	0.98	0.78	0.24	0.06
	Moderate	0.02	0.22	0.59	0.56
	Severe	0	0	0.15	0.33
	Extreme	0	0	0.03	0.06
Nakdong River	Normal	0.99	0.65	0.18	0.10
	Moderate	0.01	0.32	0.60	0.50
	Severe	0	0.03	0.20	0.30
	Extreme	0	0	0.03	0.10
Geum River	Normal	0.98	0.76	0.18	0
	Moderate	0.02	0.21	0.56	0.44
	Severe	0	0.04	0.22	0.56
	Extreme	0	0	0.04	0
Seomjin River	Normal	0.99	0.67	0.21	0
	Moderate	0.01	0.31	0.62	0.33
	Severe	0	0.02	0.15	0.44
	Extreme	0	0.01	0.02	0.22
Yeongsan River	Normal	0.99	0.68	0.17	0
	Moderate	0.01	0.29	0.63	0.40
	Severe	0	0.03	0.19	0.40
	Extreme	0	0	0.02	0.20

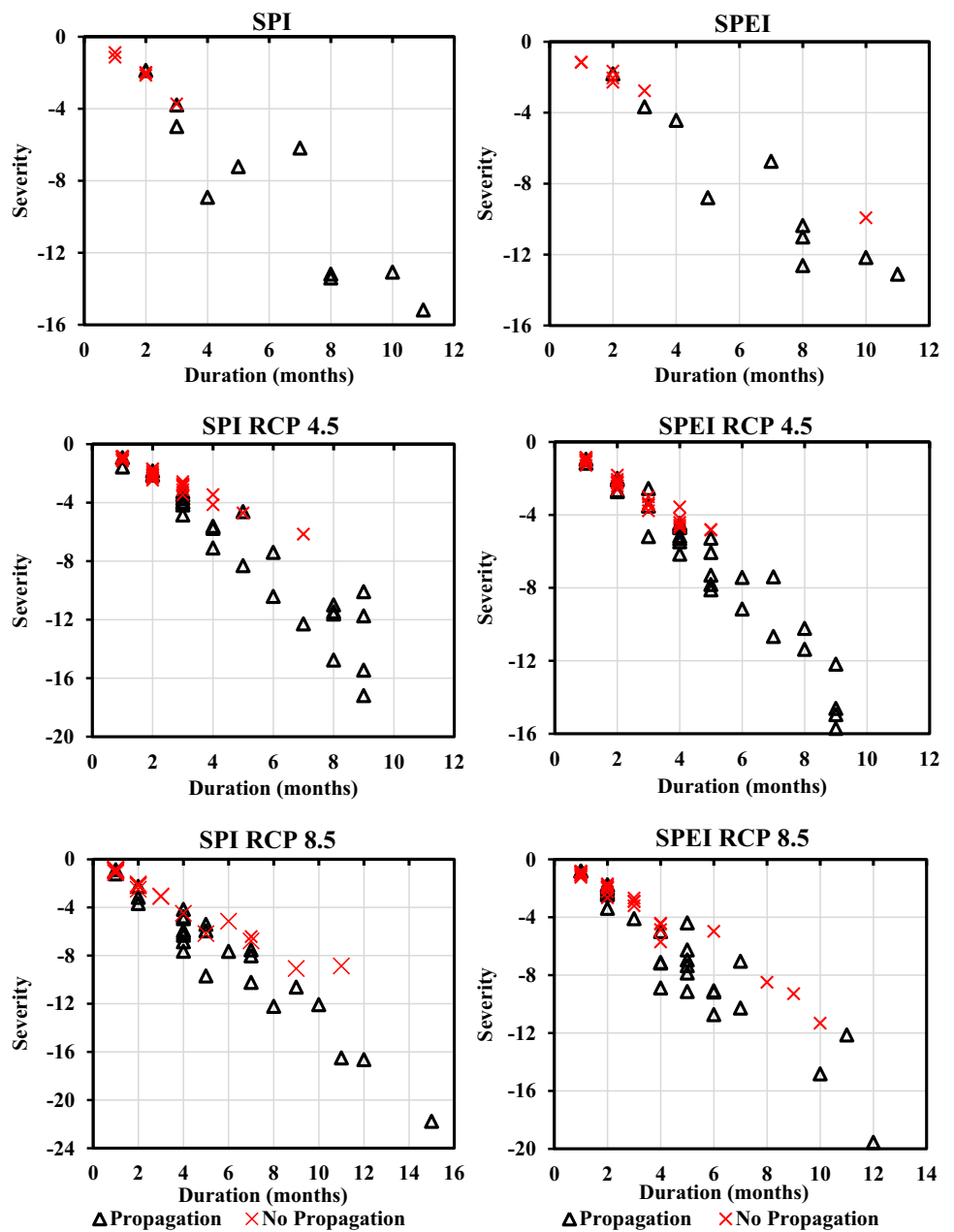
Table 7 Propagation probability of different classes of SPI into SRI under the RCP 8.5 scenario

Basin	SRI	SPI			
		Normal	Moderate	Severe	Extreme
Han River	Normal	0.97	0.69	0.12	0
	Moderate	0.03	0.31	0.63	0.29
	Severe	0	0	0.24	0.43
	Extreme	0	0	0	0.29
Nakdong River	Normal	0.98	0.68	0.17	0
	Moderate	0.02	0.29	0.74	0.18
	Severe	0	0.03	0.09	0.64
	Extreme	0	0	0	0.18
Geum River	Normal	0.98	0.64	0.12	0
	Moderate	0.02	0.33	0.77	0.20
	Severe	0	0.02	0.09	0.40
	Extreme	0	0.01	0.02	0.40
Seomjin River	Normal	0.99	0.72	0.14	0.05
	Moderate	0.01	0.25	0.78	0.40
	Severe	0	0.02	0.05	0.40
	Extreme	0	0.01	0.03	0.15
Yeongsan River	Normal	0.99	0.70	0.09	0
	Moderate	0.01	0.29	0.83	0.28
	Severe	0	0.01	0.03	0.50
	Extreme	0	0.01	0.06	0.22

Table 8 Propagation probability of different classes of SPEI into SRI under the RCP 8.5 scenario

Basin	SRI	SPEI			
		Normal	Moderate	Severe	Extreme
Han River	Normal	0.97	0.67	0.30	0.07
	Moderate	0.03	0.32	0.54	0.36
	Severe	0	0.01	0.15	0.43
	Extreme	0	0	0	0.14
Nakdong River	Normal	0.98	0.66	0.39	0
	Moderate	0.02	0.32	0.53	0.15
	Severe	0	0.01	0.08	0.69
	Extreme	0	0	0	0.15
Geum River	Normal	0.98	0.68	0.16	0
	Moderate	0.02	0.31	0.67	0.53
	Severe	0	0.01	0.16	0.16
	Extreme	0	0	0	0.32
Seomjin River	Normal	0.97	0.73	0.19	0.07
	Moderate	0.03	0.26	0.67	0.13
	Severe	0	0.01	0.12	0.47
	Extreme	0	0	0.02	0.33
Yeongsan River	Normal	0.98	0.72	0.30	0.07
	Moderate	0.02	0.28	0.55	0.14
	Severe	0	0	0.11	0.43
	Extreme	0	0	0.04	0.36

Fig. 7 Characteristics of meteorological drought that propagates into hydrological drought in the Yeongsan River Basin during the baseline and the future periods



precipitation, which propagates slowly into soil moisture drought and, finally, hydrological drought. Figure 7 shows meteorological droughts having long duration and high severity tend to propagate into hydrological droughts, and a similar trend was noted in both climate change scenarios. The probabilistic relationship between states of meteorological and hydrological droughts was constructed using the PGM. The average drought propagation probability of the extreme state of SPI resulting in severe conditions of SRI increased significantly by 55%, whereas the average probability of the extreme state of SPEI contributing to moderate conditions of SRI increased by 78% under the RCP 4.5 scenario. However the average propagation

occurrence probability of the extreme state of both SPI and SPEI resulting in the extreme state of SRI increased by 55% and 123%, respectively under the RCP 8.5 scenario.

4 Conclusions

Meteorological drought originates due to a precipitation deficit and brings about all types of droughts. It is very important to understand variation in drought characteristics and the propagation phenomenon between meteorological, agricultural, and hydrological droughts for effective drought mitigation planning in a changing climate. In this

study, two meteorological drought indices (SPI and SPEI) and a hydrological drought index (SRI) were used to represent drought severity during the baseline period and the future period according to climate change scenarios (RCP4.5 and RCP 8.5). To investigate the effects of climate change, drought characteristics such as severity, duration, and frequency were estimated at different time periods and compared with those at the baseline period. Drought characteristics vary spatially; even though they show an increasing trend in different periods under climate change scenarios.

Finally, the drought propagation probabilities of different states of meteorological drought into different states of hydrological drought were calculated under climate change scenarios using the PGM. Drought propagation probabilities of different states of drought vary spatially, but propagation probabilities of different states of meteorological drought into hydrological drought increased significantly under climate change. In this study, we presented a new approach for calculating the propagation probability of an individual state of meteorological drought into hydrological drought. This study generally discussed the effects of climate change on drought characteristics and propagation. However, hydrological drought is a very complex phenomenon which is influenced by many human activities such as dam operation, irrigation, industrialization, and urbanization. Further investigations are needed to quantify the effects of these activities on hydrological drought and propagation. The results of this study will help decision makers and water planners for preparing drought countermeasures.

Acknowledgements This study was supported by the Korea Environmental Industry & Technology Institute (KEITI) through Advanced Water Management Research Program, funded by Korean Ministry of Environment (Grant 79616). The first author would like to thank to the Higher Education Commission (HEC) and Government of Pakistan for the scholarship under the project “HRD Initiative-MS leading to Ph.D. program of faculty development for UESTPS, Phase-1, and Batch-V for Hanyang University, South Korea”.

References

- Dai A (2012) Increasing drought under global warming in observations and models. *Nat Clim Chang* 3:52–58. <https://doi.org/10.1038/nclimate1633>
- Eum HI, Cannon AJ (2017) Intercomparison of projected changes in climate extremes for South Korea: application of trend preserving statistical downscaling methods to the CMIP5 ensemble. *Int J Climatol* 37(8):3381–3397. <https://doi.org/10.1002/joc.4924>
- Ghosh S, Mujumdar PP (2007) Nonparametric methods for modeling GCM and scenario uncertainty in drought assessment. *Water Resour Res* 43(7):W07405
- Hao ZC, Hao FH, Singh VP, Ouyang W, Cheng HG (2017) An integrated package for drought monitoring, prediction and analysis to aid drought modeling and assessment. *Environ Model Softw* 91:199–209. <https://doi.org/10.1016/j.envsoft.2017.02.008>
- Huang SZ, Li P, Huang Q, Leng GY, Hou BB, Ma L (2017) The propagation from meteorological to hydrological drought and its potential influence factors. *J Hydrol* 547:184–195. <https://doi.org/10.1016/j.jhydrol.2017.01.041>
- Intergovernmental Panel on Climate Change (IPCC) (2013) Summary for policymakers. Climate change 2013. The science of climate change. Contribution of Working Group I to the fifth assessment report of the intergovernmental panel on climate change
- Lee JH, Kim CJ (2013) A multimodel assessment of the climate change effect on the drought severity–duration–frequency relationship. *Hydrol Process* 27(19):2800–2813. <https://doi.org/10.1002/hyp.9390>
- Lee H, Im ES, Bae DH (2019) A comparative assessment of climate change impacts on drought over Korea based on multiple climate projections and multiple drought indices. *Clim Dyn*. <https://doi.org/10.1007/s00382-018-4588-2>
- McKee TB, Doesken NJ, Kleist J (1993) The relationship of drought frequency and duration to time scales. In: Proceedings of the 8th conference on applied climatology. Anaheim, pp 179–184
- Melo DDCD, Wendland E (2016) Hydrological system time lag responses to meteorological shifts. *RBRH* 21(4):766–776. <https://doi.org/10.1590/2318-0331.011616083>
- Mishra V, Cherkauer KA, Shukla S (2010) Assessment of drought due to historic climate variability and projected future climate change in the midwestern United States. *J Hydrometeorol* 11(1):46–68. <https://doi.org/10.1175/2009JHM1156.1>
- Orlowsky B, Seneviratne SI (2013) Elusive drought: uncertainty in observed trends and short-and long-term CMIP5 projections. *Hydrol Earth Syst Sci* 17:1765–1781. <https://doi.org/10.5194/hess-17-1765-2013>
- Ouyang F, Zhu Y, Fu G, Lü H, Zhang A, Yu Z, Chen X (2015) Impacts of climate change under CMIP5 RCP scenarios on streamflow in the Huangnizhuang catchment. *Stoch Env Res Risk Assess* 29(7):1781–1795. <https://doi.org/10.1007/s00477-014-1018-9>
- Palmer WC (1965) Meteorological drought. US Department of Commerce, Weather Bureau, Research Paper No. 45, p 58
- Rhee J, Cho J (2016) Future changes in drought characteristics: regional analysis for South Korea under CMIP5 projections. *J Hydrometeorol* 17:437–451. <https://doi.org/10.1175/JHM-D-15-0027.1>
- Sattar MN, Kim TW (2018) Probabilistic characteristics of lag time between meteorological and hydrological droughts using a Bayesian model. *Terr Atmos Ocean Sci* 29:1–12. <https://doi.org/10.3319/TAO.2018.07.01.01>
- Shin JY, Chen S, Lee JH, Kim TW (2018a) Investigation of drought propagation in South Korea using drought index and conditional probability. *Terr Atmos Ocean Sci* 29:231–241. <https://doi.org/10.3319/TAO.2017.08.23.01>
- Shin Y, Lee Y, Choi J, Park JS (2018b) Integration of max-stable processes and Bayesian model averaging to predict extreme climatic events in multi-model ensembles. *Stoch Env Res Risk Assess* 33(1):47–57. <https://doi.org/10.1007/s00477-018-1629-7>
- Shukla S, Wood AW (2008) Use of a standardized runoff index for characterizing hydrologic drought. *Geophys Res Lett* 35(2):L02405. <https://doi.org/10.1029/2007GL032487>
- Stagge JH, Tallaksen LM, Gudmundsson L, Van Loon AF, Stahl K (2015) Candidate distributions for climatological drought indices (SPI and SPEI). *Int J Climatol* 35(13):4027–4040. <https://doi.org/10.1002/joc.4267>
- Tsakiris G, Vangelis H (2005) Establishing a drought index incorporating evapotranspiration. *Eur Water* 9(10):3–11

- Van Loon AF, Van Lanen HAJ (2012) A process-based typology of hydrological drought. *Hydrol Earth Syst Sci* 16:1915–1946. <https://doi.org/10.5194/hessd-8-11413-2011>
- Van-Rooy MP (1965) A rainfall anomaly index (RAI) independent of time and space. *Notos* 14:43–48
- Vicente-Serrano SM, Beguería S, López-Moreno JI (2010) A multiscalar drought index sensitive to global warming: the standardized precipitation evapotranspiration index. *J Clim* 23:1696–1718. <https://doi.org/10.1175/2009jcli2909.1>
- Wang W, Ertsen MW, Svoboda MD, Hafeez M (2016a) Propagation of drought: from meteorological drought to agricultural and hydrological drought. *Adv Meteorol*. <https://doi.org/10.1155/2016/6547209>
- Wang X, Yang T, Li X, Shi P, Zhou X (2016b) Spatio-temporal changes of precipitation and temperature over the Pearl River basin based on CMIP5 multi-model ensemble. *Stoch Env Res Risk Assess* 31(5):1077–1089. <https://doi.org/10.1007/s00477-016-1286-7>
- Wilhite DA, Glantz MH (1985) Understanding the drought phenomenon: the role of definitions. *Water Int* 10(3):111–120. <https://doi.org/10.1080/02508068508686328>
- Wu J, Miao C, Zheng H, Duan Q, Lei X, Li H (2018) Meteorological and hydrological drought on the Loess Plateau, China: evolutionary characteristics, impact, and propagation. *J Geophys Res Atmos* 123(20):11–569. <https://doi.org/10.1029/2018JD029145>
- Xu K, Wu C, Hu BX (2018) Projected changes of temperature extremes over nine major basins in China based on the CMIP5 multimodel ensembles. *Stoch Env Res Risk Assess* 33(1):321–339. <https://doi.org/10.1007/s00477-018-1569-2>
- Yu Z, Gu H, Wang J, Xia J, Lu B (2017) Effect of projected climate change on the hydrological regime of the Yangtze River Basin, China. *Stoch Env Res Risk Assess* 32(1):1–16. <https://doi.org/10.1007/s00477-017-1391-2>
- Yuan X, Zhang M, Wang L (2016) Understanding and seasonal forecasting of hydrological drought in the anthropocene. *Hydrol Earth Syst Sci Dis*. <https://doi.org/10.5194/hess-2016-592>
- Zhao L, Lyu A, Wu J, Hayes M, Tang Z, He B, Liu J, Liu M (2014) Impact of meteorological drought on streamflow drought in Jinghe River Basin of China. *Chin Geogr Sci* 24:694–705. <https://doi.org/10.1007/s11769-014-0726-x>
- Zhensheng Y, Yuguo D (1990) *Climate statistics*. Meteorological Press, Beijing (in Chinese)

Publisher's Note Springer Nature remains neutral with regard to jurisdictional claims in published maps and institutional affiliations.